

## Electronic Structure and Properties of NbS<sub>3</sub> and Nb<sub>3</sub>S<sub>4</sub>

D. W. BULLETT\*

*Cavendish Laboratory, Madingley Road, Cambridge, CB3 0HE, United Kingdom*

Received March 13, 1979; in final form July 27, 1979

Electronic structure calculations for NbS<sub>3</sub> and Nb<sub>3</sub>S<sub>4</sub> are reported. The NbS<sub>3</sub> structure is closely related to that of ZrSe<sub>3</sub>. In the undistorted ZrSe<sub>3</sub> atomic arrangement, NbS<sub>3</sub> would be a metal; it is shown that the observed distortion, a pairing of Nb atoms along the *b*-axis relative to ZrSe<sub>3</sub>, stabilizes the NbS<sub>3</sub> crystal by inducing a 0.5-eV semiconducting gap. Nb<sub>3</sub>S<sub>4</sub> is found to be a metal with the Fermi level lying near a deep minimum in the density of electron states.

### Introduction

This paper presents the continuation of a study (1, 2) of transition metal trichalcogenides MX<sub>3</sub> (*M*: Ti, Zr, Hf, Nb, Ta; *X*: S, Se, Te). The structural feature characteristic of this class of compounds is the bicapped trigonal prismatic coordination of chalcogens around each metal atom. Successive trigonal prisms share their triangular faces, leading to infinite chains along the *b*-axis. Chalcogens on neighboring chains cap two of the rectangular faces of each prism to provide a weak bonding between chains. Two of the chalcogen atoms in the base of each trigonal prism are closely bonded.

However, transport properties within this family vary widely. In Refs. (1) and (2) it was shown that apparently small differences in the arrangement of the prismatic chains in different selenides lead to radically different energy bands which account for the observed properties. In particular, ZrSe<sub>3</sub> was shown to be a semiconductor with a gap of 1.5 eV between occupied and unoccupied states, whereas NbSe<sub>3</sub> and TaSe<sub>3</sub> were predicted to

be highly anisotropic metals. Additionally, the charge-density wave transitions which have been observed experimentally in NbSe<sub>3</sub> (3-6) were revealed as a consequence of the pseudo-one-dimensional Fermi surface; no such one-dimensional behavior occurs in the TaSe<sub>3</sub> energy bands (2) and no charge-density waves have been observed in this compound.

### Crystal Structure of NbS<sub>3</sub>

The crystal structure of NbS<sub>3</sub> has been fully determined very recently by Rijnsdorp and Jellinek (7), following preliminary studies by Kadijk and Jellinek (8), and by Grigoryan and Novoselova (9). The unit cell is similar to that of ZrSe<sub>3</sub> (10), but with a doubling of the *b*-axis (Fig. 1). The main deviation from a ZrSe<sub>3</sub>-type structure is a displacement of the metal atoms by 0.16 Å from the centers of the coordination polyhedra to form Nb-Nb pairs along the *b*-axis. Without this distortion, it is clear from our investigation of ZrSe<sub>3</sub> (2) that NbS<sub>3</sub> would be metallic. The extra electrons introduced by changing from a group IV to a group V transition element would have to be

\* Present address: School of Physics, University of Bath, Bath, England.

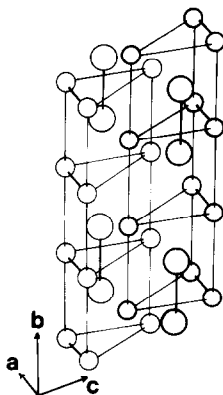


FIG. 1. Schematic picture of the  $\text{NbS}_3$  structure. Eight S atoms (small circles) form a bicapped trigonal prism around Nb atoms (large circles). Metal-metal bonds occur parallel to the  $b$ -axis.

accommodated in the conduction band. In fact  $\text{NbS}_3$  forms as black needles and displays the properties of a diamagnetic semiconductor (7-9). It is interesting to see how the pairing of Nb atoms leads to these effects in an electronic structure calculation.

### Electronic Structure of $\text{NbS}_3$

The computational method was the same as that of Refs. (1) and (2). Electron states were calculated by an atomic orbital method, using a basis of chalcogen  $s$ - and  $p$ -orbitals and  $s$ -,  $p$ -, and  $d$ -orbitals on the metal atoms. The dimension of the secular matrix was then  $(84 \times 84)$ . There are no empirical parameters in the method. The two-centered matrix elements between undistorted atomic orbitals were evaluated explicitly in a crystal potential obtained from overlapping atomic charge densities. All three-centered effects were neglected. The same method has been very successful in describing the properties of the layered dichalcogenides (11).

The energy levels calculated for the isolated S and Nb atoms are shown in Table I. The position of the  $d$ -level of a transition element atom depends quite sensitively on the configuration of the other electrons; the

TABLE I  
ENERGY LEVELS OF ISOLATED  
ATOMS (eV)

|     | Nb ( $s^{0.7} p^{0.5} d^{3.8}$ ) | S ( $s^2 p^4$ ) |
|-----|----------------------------------|-----------------|
| $s$ | -5.3                             | -17.8           |
| $p$ | -3.0                             | -8.0            |
| $d$ | -4.4                             |                 |

$d$ -occupation adopted here for the Nb atom was found to be consistent with the  $d$ -component of the ground state charge density in the dichalcogenide calculations (11).

The resulting density of states as a function of energy for electrons in  $\text{NbS}_3$  is displayed in Fig. 2. Many features are reminiscent of  $\text{ZrSe}_3$  (2). In each case the energy spectrum separates broadly into three parts, which we may loosely label (in order of decreasing binding energy) as chalcogen  $s$ -, chalcogen  $p$ -, and metal  $d$ -bands, respectively. These labels denote only the major component of the eigenstates in a particular band. The bonding in these compounds is provided by strong hybridization between  $p$ - and  $d$ -states, and the statement that most " $p$ -states" are filled while all " $d$ -states" are empty does not imply that there is a large transfer of electrons from transition metal atoms to chalcogens.

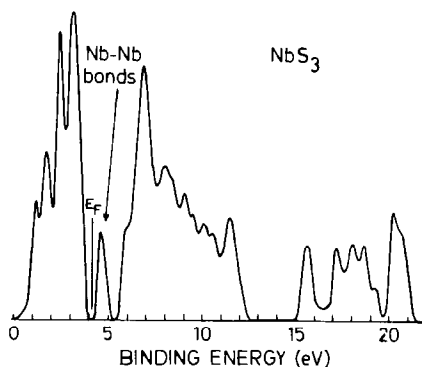


FIG. 2. Valence band density of states of  $\text{NbS}_3$  (smoothed by a Gaussian of half-width  $\sigma = 0.15$  eV).

The *s*-bands in ZrSe<sub>3</sub> form three subbands as a consequence of the bonding and antibonding levels of the two closely spaced Se atoms being pushed below and above the *s*-level of the third Se atom in the triangular base of each prism. A similar effect may be seen in the *s*-bands of NbS<sub>3</sub>, though in this case, because of the lower crystal symmetry the division is less marked and the nonbonding and antibonding bands overlap.

The semiconducting gap of 1.5 eV in the calculated spectrum of ZrSe<sub>3</sub> occurs after eight "*p*-bands" per formula unit have been doubly occupied. The experimentally observed gap is 1.8 eV (12). This gap comes after eight and not nine bands because the ninth *p*-band would be the antibonding component of the closely bonded Se–Se pairs and lies up in the conduction band. It is in this semiconducting gap that the main distinction between the ZrSe<sub>3</sub> and NbS<sub>3</sub> densities of states can be seen. Nb–Nb pairing along the *b*-axis pulls one "metal *d*-band" down by splitting one of the conduction bands into bonding and antibonding subbands. Occupation of the lower subband stabilizes the structure at a Nb–Nb spacing of 3.04 Å. The nearest-neighbor interaction between *d*<sub>z<sup>2</sup>-orbitals (where *z* is the direction of the *b*-axis) is then –0.8 eV. The result is an energy gap of 0.5 eV above the highest occupied band. Thus the electronic structure investigation accounts naturally for the semiconducting properties and black needle-like appearance of NbS<sub>3</sub> crystals.</sub>

### Nb<sub>3</sub>S<sub>4</sub>

For completeness, the electronic structure resulting from a similar investigation of Nb<sub>3</sub>S<sub>4</sub> is also presented here. Nb<sub>3</sub>S<sub>4</sub> may be prepared in needle-shaped crystals from the elements at 1000–1300°C, using iodine as a carrier in a vapor transport reaction (13). The crystal lattice is hexagonal (space group *P*6<sub>3</sub>/*m*) and the atomic arrangement is isotopic with Nb<sub>3</sub>S<sub>4</sub> and Nb<sub>3</sub>Te<sub>4</sub> (14). The

structure (Fig. 3) is built up from NbS<sub>6</sub> octahedra, linked by shared faces and edges. There are some similarities to the NbS<sub>3</sub> structure: each metal atom is displaced from the center of the coordinating octahedron toward one of the faces, so that zigzag Nb–Nb–Nb chains are formed running along the *c*-direction (which is also the needle axis). The Nb–Nb distances within these chains are again comparable to those in metallic Nb. There are no close S–S approaches.

The resulting electronic density of states of Nb<sub>3</sub>S<sub>4</sub> is displayed in Fig. 4. The interpretation of bands is less simple because the geometrical structure is much more complicated than that of the trisulfide. There are two types of S environment in the unit cell: two S(1) sites each surrounded by six Nb neighbors in a trigonal prism, and six S(2) sites with very asymmetric surroundings formed by four Nb atoms. Sulfur *s*-states form a peak at –19 eV. Nb–S bonding states, or "*p*-bands," form the broad band of states at energies between –6 and –12 eV; the corresponding Nb–S antibonding states lie unoccupied at higher energies of –1 to –3.5 eV. The remaining *d*-orbital contributions may be loosely classified as nonbonding with respect to the octahedral directions of the coordinating S atoms, and form states of very complicated hybridization between the bonding and antibonding peaks. In parti-

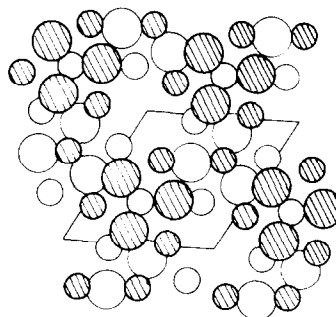


FIG. 3. The crystal structure of Nb<sub>3</sub>S<sub>4</sub>, projected along the *c*-axis. Nb atoms are denoted by large circles, S by small circles. Atoms at  $z = \frac{3}{4}$  are hatched, and those at  $z = \frac{1}{4}$  are open. The unit cell is outlined.

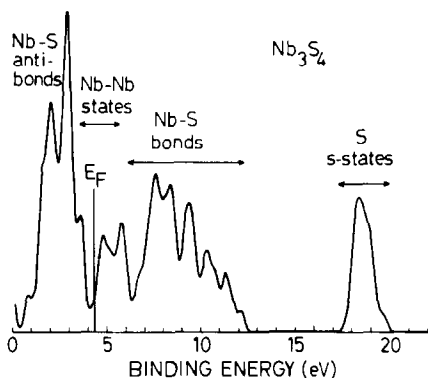


FIG. 4. Valence band density of states of  $\text{Nb}_3\text{S}_4$ .

cular, the close approaches of Nb atoms along zigzag chains parallel to the  $c$ -axis lead to three quasi-one-dimensional bands each of width  $\sim 1.5$  eV in which the charge density is almost entirely located on the Nb atoms. The conduction electron number is sufficient to fill only one-third of this group of bands. Thus  $\text{Nb}_3\text{S}_4$  has metallic properties rather akin to those of  $\text{NbSe}_3$  (2).

We note how both the  $\text{NbSe}_3$  and  $\text{Nb}_3\text{S}_4$  structures are stabilized by adopting an atomic configuration in which the Fermi level  $E_F$  lies close to a deep minimum in the density of states. Indeed, the room temperature resistivities of  $\text{Nb}_3\text{S}_4$  (13) and  $\text{NbSe}_3$  (4) are quite similar ( $\sim 10^{-4}$  ohm-cm).

## References

1. D. W. BULLETT, *Solid State Commun.* **26**, 563 (1978).
2. D. W. BULLETT, *J. Phys. C* **12**, 277 (1979).
3. P. MONCEAU, N. P. ONG, A. M. PORTIS, A. MEERSCHAUT, AND J. ROUXEL, *Phys. Rev. Lett.* **37**, 602 (1976).
4. J. CHAUSSY, P. HAEN, J. C. LASJAUNIAS, P. MONCEAU, G. WAYSAND, A. WAIN TAL, A. MEERSCHAUT, P. MOLINIÉ, AND J. ROUXEL, *Solid State Commun.* **20**, 759 (1976).
5. P. MONCEAU, J. PEYRARD, J. RICHARD, AND P. MOLINIÉ, *Phys. Rev. Lett.* **39**, 161 (1977).
6. J. L. HODEAU, M. MAREZIO, C. ROUCAU, R. AYROLES, A. MEERSCHAUT, J. ROUXEL AND P. MONCEAU, *J. Phys. C* **11**, 4117 (1978).
7. J. RIJNSDORP AND F. JELLINEK, *J. Solid State Chem.* **25**, 325 (1978).
8. F. KADIJK AND F. JELLINEK, *J. Less Common Metals* **19**, 421 (1969).
9. L. A. GRIGORYAN AND A. V. NOVOSELOVA, *Dokl. Akad. Nauk SSSR* **144**, 795 (1962).
10. W. KRÖNERT AND K. PLIETH, *Z. Anorg. Allg. Chem.* **336**, 207 (1965).
11. D. W. BULLETT, *J. Phys. C* **11**, 4501 (1978).
12. W. SCHAIRER AND M. W. SCHAFFER, *Phys. Status Solidi A* **17**, 181 (1973); F. JELLINEK, R. A. POLLAK, AND M. W. SCHAFFER, *Mater. Res. Bull.* **9**, 845 (1974).
13. A. F. J. RUYSSINK, F. KADIJK, A. J. WAGNER, AND F. JELLINEK, *Acta Crystallogr. Sect. B* **24**, 1614 (1968).
14. K. SELTE AND A. KJEKSHUS, *Acta Crystallogr.* **17**, 1568 (1964).